



biblio.ugent.be

The UGent Institutional Repository is the electronic archiving and dissemination platform for all UGent research publications. Ghent University has implemented a mandate stipulating that all academic publications of UGent researchers should be deposited and archived in this repository. Except for items where current copyright restrictions apply, these papers are available in Open Access.

This item is the archived peer-reviewed author-version of:

Title: Evaluation of in-line spatial filter velocimetry as pat monitoring tool for particle growth during fluid bed granulation

Authors: Burggraeve A., Van Den Kerhof T., Hellings M., Remon J.P., Vervaet C., De Beer T.

In: European Journal of Pharmaceutics and Biopharmaceutics, 76(1), 138-146 (2010)

Optional: link to the article

To refer to or to cite this work, please use the citation to the published version:

Authors (year). Title. *journal Volume(Issue)* page-page. Doi: 10.1016/j.ejpb.2010.06.001

EVALUATION OF IN-LINE SPATIAL FILTER VELOCIMETRY AS PAT MONITORING TOOL FOR PARTICLE GROWTH DURING FLUID BED GRANULATION

A. Burggraeve^a, T. Van Den Kerkhof^b, M. Hellings^b, J.P. Remon^c, C. Vervaet^c, T. De Beer^a

^aLaboratory of Pharmaceutical Process Analytical Technology, Department of Pharmaceutical Analysis, Ghent University, Harelbekestraat 72, B-9000 Ghent, Belgium

^bJohnson & Johnson Pharmaceutical Research and Development, Analytical Development, Beerse, Belgium

^cLaboratory of Pharmaceutical Technology, Department of Pharmaceutics, Ghent University, Harelbekestraat 72, B-9000 Ghent, Belgium

Abstract

In this study, the feasibility of spatial filter velocimetry (SFV) as Process Analytical Technology tool for the in-line monitoring of the particle size distribution during top spray fluidized bed granulation was examined. The influence of several process (inlet air temperature during spraying and drying) and formulation variables (HPMC and Tween 20 concentration) upon the particle size distribution during processing, and the end product particle size distribution, tapped density and Hausner ratio was examined using a design of experiments (DOE) (2-level full factorial design, 19 experiments). The trend in end granule particle size distributions of all DOE batches measured with in-line SFV was similar to the off-line laser diffraction (LD) data. Analysis of the DOE results showed that mainly the HPMC concentration and slightly the inlet air temperature during drying had a positive effect upon the average end granule size. The in-line SFV particle size data, obtained every 10 s during processing, further allowed to explain and better understand the (in)significance of the studied DOE variables, which was not possible based on the LD data as this technique only supplied end granule size information. The variation in tapped density and Hausner ratio among the end granules of the different DOE batches could be explained by their difference in average end granule size. Univariate, multivariate PLS and multiway N-PLS models were built to relate these end granule properties to the in-line measured particle size distribution. The multivariate PLS tapped density model and the multiway N-PLS Hausner ratio model showed the highest R^2 values in combination with the lowest RMSEE values (R^2 of 82% with an RMSEE of 0.0279 for tapped density and an R^2 of 52% with an RMSEE of 0.0268 for Hausner ratio, respectively).

Keywords

Spatial Filter Velocimetry (SFV), Process Analytical Technology (PAT), fluid bed granulation, particle size (distribution), process understanding, in-line measurements

1. Introduction

Fluid bed granulation is an extensively used process within the pharmaceutical industry to improve powder properties (i.e., flowability, compressibility, ...) for downstream processing (e.g., tableting, ...). During fluid bed granulation, a liquid binder is sprayed onto particles of a powder mixture, circulating through the fluidized bed. As a result, these primary powder mixture particles collide with each other, hence forming larger permanent aggregates (granules), in which the original particles are still identifiable [1].

The concept of Process Analytical Technology (PAT) has been introduced by the American Food and Drug Administration. The general idea is that *quality cannot be tested into products; it should be built-in or should be by design* [2-3]. Through the identification and understanding of critical process and formulation parameters, one should be able to completely control the manufacturing processes, hence constantly ensuring a predefined end product quality. To enable the implementation of this scientific and risk-based framework in pharmaceutical production processes, a combination of suitable PAT tools is needed, such as modern process analyzers for process and endpoint monitoring, chemometrics, control tools, continuous improvement and knowledge management tools.

PAT implementation in pharmaceutical production processes may lead to increased process understanding, continuous process monitoring of critical information, process control, reduced production cycle time, prevention of rejects and reprocessing, and real time release.

Particle size distribution is one of the key characteristics of a granulated product. Inappropriate particle size distribution influences granule properties as density, powder flowability and dustiness which in turn might cause problems during further processing. Hence, understanding and control of the granule growth mechanism during granulation are of major importance.

Sieve analysis, image analysis and laser diffraction are the traditional off-line techniques used for granule size determination. These methods can be time-consuming and labour intensive (sample preparation) and do not supply in-process information. As a result, research has been done on at-line, on-line and in-line particle size measuring tools. The use of on-line *image analysis* for granule size determination was initiated by Watano et al. [4-9] and more recently investigated by Naervanen et al. [10]. As a *near infrared (NIR)* spectrum is dependent on the chemical and physical composition and properties of a measured sample, NIR has been extensively investigated for the fast and non-destructive (at-line, on-line or in-line) particle size monitoring during granulation, usually combined with moisture content determination [11-16]. A couple of reports can be found on the application of *focused beam reflectance measurements (FBRM)* in-line or at-line during fluid bed granulation [15,17]. Tok et al. describe the combined use of FBRM, NIRS and acoustic emission measurements in a pilot-scale fluidized bed granulation process [15]. In-line FBRM and NIRS probes were able to detect the three granulation rate processes to varying degrees of sensitivity due to fouling. Although an anti-static spray was applied onto the surface of the probe windows, FBRM and NIR signals remained susceptible to fouling during granulation. More recently, FBRM probes equipped with a scraper system designed for removing agglomerates of the probe window in cohesive particle conditions were developed (FBRM[®] C35 technology). The use of *acoustic emission spectroscopy* in granulation has also been described [15, 18-21]. As this is a non-intrusive technique, it has the advantage of not

interfering with the fluidizing bed. However, the technique's sensitivity can be highly affected by the fluidizing air flow rate and external uncontrollable factors.

Spatial filter velocimetry (SFV) is a method similar to FBRM as they both use chord length distribution to express granule size. Both techniques project a laser beam onto the moving particles. However, FBRM uses the backscattered light and converts it to size measurement, while SFV uses the generated shadow. During SFV measurements, particles pass through a laser beam and cast shadows onto a linear array of optical fibres. In that way, a burst signal is generated, which is proportional to particle velocity. As the particles pass through the beam, a secondary pulse is generated by a single optical fibre. Knowing the time of the pulse and the velocity of the moving particles, the chord length can be calculated. The measurement cell of the SFV probe is equipped with sapphire windows that are kept clean through the use of an internal compressed air supply system, which prevents fouling of the windows. The internal airflow also ensures the dispersion of highly concentrated particles and optimizes the movement of these particles through the measurement zone. The measurement results are reported in various ways, e.g. sieve distribution (as fraction and passage), volume distribution, number distribution, velocity distribution, ... [22-24]. Närvänen et al. compared three different particle size measurement techniques: sieve analysis, laser diffraction and off-line SFV to model process parameters of a fluid bed granulation process [25]. The SFV results were the most consistent among the three studied techniques. Another study by the same group showed that the in-line particle size data measured via SFV could be used to monitor different process phenomena and process failure [26]. However, particle size determination was influenced by size segregation in the fluid bed: the in-line technique underestimated and the at-line method overestimated the final granule size. Lipsanen et al. showed that the pressure difference over the upper filters (indication of blockage of filters) and the fluidization parameter correlated well with the in-line particle size measurements [27].

In the present study, SFV was evaluated as PAT tool for the in-line particle size monitoring in a pharmaceutical fluid bed granulation process. A design of experiments (DOE) was performed to study the influence of different process and formulation variables upon the average granule size and the granule size distribution (response variables), measured in-line with SFV, and compared to off-line laser diffraction results. It was also examined whether the continuously obtained in-line SFV data could improve our understanding about the impact of the DOE variables on the fluidized bed granulation process. Furthermore, we examined whether the in-line particle size data could be related to off-line measured end granule properties (tapped density and Hausner ratio) using univariate, multivariate and multiway models, hence allowing early estimation of these end product properties during processing.

Whereas previous reports about in-line SFV emphasized on the sensitivity of the technique towards the in-line detection of granule size and process failures [26-27], the present study examines the application of the technique to enhance fluidized bed process understanding through the continuous measurement of particle size, in combination with DOE. Furthermore, models were built using the continuously measured in-line particle size information allowing early prediction of end granule properties.

2. Materials and methods

2.1 Materials

Each batch, consisting of dextrose monohydrate (700 g, Roquette Frères, Lestrem, France) and unmodified maize starch (Cargill Benelux, Sas van Gent, The Netherlands), was granulated with an aqueous binder solution of HPMC (type 2910 15 mPa.s, Dow Chemical Company, Plaquemine-LA, USA) and Tween 20 (Croda Chemicals Europe, Wilton). The amount of HPMC and Tween 20 in the granules was varied according to the DOE (section 2.4). HPMC was always sprayed as a 4% solution and the total amount of solids was kept constant at 1000 g (amount of maize starch was varied accordingly).

2.2 Fluid Bed Granulation

Granulation was performed in a laboratory scale fluid bed granulator (GPCG 1, Glatt, Binzen, Germany). A top spray nozzle with a diameter of 1.2 mm was installed at a height of 26 cm from the distributor plate, and an atomization pressure of 1 bar was used during all experiments. The pump was set at a feed rate of 16 g/min. Shaking of the filter bags was necessary every 45 s for a period of 7 s, to prevent the entrapment of small particles in the bags. Through visual monitoring of the flowing powder bed, the inlet airflow rate was adjusted when necessary to keep the height of the fluidized bed constant. The inlet air temperature during spraying and drying was varied according to the DOE. Granules were dried until an outlet air temperature of 37°C and a product temperature of 45°C was obtained (granulation endpoint).

2.3 In-line measurements with Spatial Filter Velocimetry probe

An in-line spatial filter velocimetry probe (Parsum IPP 70; Gesellschaft für Partikel-, Strömungs- und Umweltmesstechnik, Chemnitz, Germany) was installed in the fluid bed granulator at a height of 20 cm and at approximately 5 cm from the sidewall of the granulator (i.e., between the sidewall of the granulator and the outer part of the spray cone, figure 1). If the probe was placed in the centre of the fluid bed (i.e., below the spray cone), probe fouling by the moist product occurred. Using an internal (20 L/min) and external (3 L/min) air connection, the granules were directed through an aperture (4 mm diameter), to ensure the dilution of the product mass (avoidance of aperture obstruction) and to prevent back flush of the measured granules. Measured raw data were collected via an A/D converter and led to a computer. The In-line Particle Probe V7.12a software operated in the Windows XP environment. SFV measurements started and stopped simultaneously with the start and end of fluidization, respectively. During the entire granulation process, SFV data were collected every second, but an average granule size distribution was saved every 10 s.

2.4 Design of experiments

A 2-level full factorial design containing 4 variables (*HPMC concentration, Tween 20 concentration, inlet air temperature during spraying and inlet air temperature during drying*, table 1) and three center point repetition experiments was performed. In total, 19

experiments were carried out to evaluate the influence of the examined variables and their interactions upon the average particle size and particle size distribution during granulation within the defined knowledge space (table 2). All granulation batches were performed in a randomized order.

2.5 Characterization of granules

After manufacturing, the average particle size, particle size distribution, tapped density and Hausner ratio of the end product of each batch was determined.

A 20 g sample was measured with *laser diffraction (LD)* (Mastersizer S long bench, Malvern Instruments, Malvern, UK). The dry powder dispersing unit was used with a jet pressure of 0.2 bar and a measurement time of 20 s. This low dispersing pressure was selected to prevent the breaking up of the granules. All measurements were performed in triplicate and the particle size distributions were characterized via their $D(v, 0.1)$, $D(v, 0.5)$ and $D(v, 0.9)$ values (10, 50 or 90% of the distribution has a particle size smaller than this value).

Tapped density of the granules was determined as described in the European Pharmacopoeia 6.5. A graduated cylinder of 100 mL was used and samples were tapped 1250 times. All density measurements were performed in triplicate and the average density is reported.

Powder flow characteristics were predicted by calculation of Hausner ratio values, according to the European Pharmacopoeia 6.0 and determined in triplicate.

2.6 Data analysis

Analysis of the DOE results was performed with MODDE software (Version 8.0.2, Umetrics, Umeå, Sweden) and Microsoft Excel 2007.

Partial least squares (PLS) models were developed using SIMCA-P+ software (Version 12.0.1, Umetrics, Umeå, Sweden). Matlab 7.1 (The MathWorks, Inc., Natick, MA) with the PLS Toolbox for MATLAB version 4.2 was used for N-way PLS modeling.

3. Results and Discussion

3.1 Comparison between in-line SFV and off-line LD results

In a first instance it was investigated if the end granule particle size determined by in-line SFV corresponded to the off-line LD results for all DOE batches. Although the measurement principles of both techniques are different (LD assumes spherical particles, SFV does not), similar trends in particle size distributions should be observed. Batches with a small/large particle size should be classified by both techniques as small/large. The SFV volume particle size distribution was used for comparison and the average of the in-line measured particle size during the last granulation process minute (i.e., 6 data points) was used. Each batch was measured in triplicate with LD and the average particle size was calculated. D_{10} , D_{50} and D_{90} values of LD and SFV data demonstrated a similar pattern (only the D_{50} values of both techniques are shown).

Figure 2 shows that an identical trend in D_{50} values between all 19 DOE batches was obtained by the two particle sizing techniques. However, the D_{50} values measured with SFV

were always higher than those obtained using LD. An explanation for this observation might lay in the LD measurement technique. Using the dry powder dispersing unit, the particles experience rapid accelerations as the air stream passes through a venturi. Due to the high shear applied during this process and the subsequent collisions with the wall of the apparatus, some granules may break or crumble. During the SFV measurements, pressurized air was also used for dispersing the granules, however the particles passed directly through the measurement zone. No collisions occurred as no high shear was applied.

Confirmation of this hypothesis can be found in figure 3, which shows the differences between the D10, D50 and D90 results of the SFV and LD measurements for the 19 DOE batches. This figure demonstrates that the D90 differences are larger for most batches compared to the D10 and D50 differences. During the LD measurements, the fragile granules collided with the wall and broke up into smaller particles, which corresponded to a particle size in the range of the D10 and D50 values. As a consequence, the D10 and D50 SFV-LD differences were smaller compared to the D90 differences.

This hypothesis was also confirmed by the particle size measurements of low friable spherical granules (i.e., pellets, Cellets[®] 100, 200 and 350, Pharmatrans Sanaq Pharmaceuticals, Basel, Switzerland). The particle size of the Cellets[®] was measured using SFV and LD under the same software settings and experimental setup as during the DOE granule measurements. As these Cellets[®] have a low friability, the differences between the D10, D50 and D90 values of SFV and LD respectively did not increase due to attrition during LD measurement, in contrast to observations obtained for the 'breakable' granules. Moreover, the differences between the D-values are negative or positive, indicating this difference is random.

Besides the LD measurement technique, the assumption of spherical particles during LD measurements might be an additional factor contributing to the discrepancy between SFV and LD values. Especially for larger particles, the effect of these different measurement principles could be expected to be more pronounced as their particle shape will deviate more distinct from a sphere.

Närvänen et al. reported significant differences between the in-line SFV and off-line LD measured particle size, when larger granules (>200 μm) were formed during granulation (in-line data underestimated the actual particle size) [26]. They explained that size segregation was occurring during fluidization. Hence, a high amount of larger granules was present in the lower part of the fluid bed chamber and a high amount of smaller granules was present in the upper part of the chamber. As a result, the largest particles could not reach the SFV probe which was placed in the upper part of the fluid bed chamber and were hence not measured. According to figures 4a and 4b, the in-line SFV data did not underestimate the actual particle size due to size segregation for our study. These figures present the difference in D50 values between the SFV and LD results for the 19 DOE batches, arranged according to increasing SFV end granule size (figure 4a) and increasing LD end granule size (figure 4b) in the x-axes, respectively. If size segregation would have occurred, these differences should increase according to increasing end granule size (i.e., in function of x-axis), which is clearly not the case in both figures.

These primary results suggest that although there is a systematic difference between LD and SFV data due to the granule break-up during the LD measurements, the SFV technique adequately describes the actual particle size distribution during processing.

3.2 DOE analysis

3.2.1 Comparison between in-line SFV and off-line LD DOE results

The average D50 value obtained during the last minute of drying (i.e., 6 data points) was used as SFV response value. LD measurements of the end granules were performed in triplicate and the average D50 value was used as LD response. For each of these responses, a DOE regression model was calculated. Using the MODDE software the raw data were in first instance evaluated by means of a replicate plot and a descriptive statistics plot in which outliers could be identified. Subsequently a Multiple Linear Regression model was fitted and the corresponding parameters: goodness of fit (R^2) and goodness of prediction (Q^2) were evaluated. The least significant model terms were excluded provided that Q^2 increased. R^2 and Q^2 values and the significant examined variables can be found in tables 3 and 4, respectively.

According to table 3, R^2 and Q^2 values of the SFV and LD model are very similar and indicate a good model. Both models also show the same significant factors (table 4): *HPMC concentration (positive effect upon particle size), inlet air temperature during drying (positive effect upon particle size) and the interaction between these factors (positive effect upon particle size)*. Although the HPMC concentration was the most significant variable, exclusion of T_{drying} and $\text{HPMC} \cdot T_{\text{drying}}$ (in the LD model this latter coefficient has a p-value larger than 0.05, table 4) was not done as this resulted in lower R^2 and Q^2 values. Use of the D10 and D90 values of SFV and LD measurements as responses resulted in the same conclusions. The width ($(D90 - D10)/D50$) of the particle size distribution was similar for all DOE batches.

Normal probability plots or half-normal plots are another tool to identify significant effects. Normally distributed non-significant effects form a straight line through zero in these plots, while significant effects deviate from this pattern. Development of these plots was done as described in Vander Heyden et al. [28]. Applying the algorithm of Dong, a numerical limit value was obtained which could be plotted onto the half-normal plot and allowed a more objective quantitative identification of the significant effects: effects larger than the calculated margin of error (ME) are considered as significant.

Both half-normal plots (figures 5a and 5b) point out the same conclusion: all effects lie on a straight line except for effect A (HPMC concentration) and only effect A is larger than the margin of error, indicating this was a significant effect. However, both plots also show that effect D (inlet air temperature during drying) is the second most important effect, but classified as a borderline case as its value is below the margin of error.

3.2.2 Explanation of the (in)significance of the DOE factors based on in-line SFV data

As granule growth information was obtained every 10 seconds during granulation using SFV, this in-process information allows thorough explanation and better understanding of the (in)significance of the examined process and formulation variables.

Influence of HPMC concentration

According to DOE analysis, larger granules are produced by increasing the HPMC amount. These results are in accordance with the well known adhesive and cohesive properties of HPMC in granule formation. Figure 6 shows the influence of HPMC concentration on the granulation process for batches 13 and 14, containing 1% and 3% HPMC, respectively. The other settings are the same for both batches. The in-line data revealed that the increase in particle size was actually due to 2 effects:

1. Spraying more binder liquid resulted in larger particles immediately after spraying the binding liquid (i.e. before the start of drying). After spraying, batch 13 has a particle size of 200 μm and batch 14 a particle size of 415 μm .
2. Increasing the HPMC concentration created less friable granules, producing less fines during the drying period. Batch 13 has a decrease in particle size of approximately 60 μm during drying, while batch 14 decreases only 25 μm in particle size during drying.

Influence of inlet air temperature during drying

The DOE results indicated that an increase in drying temperature resulted in larger granules, but the significance of this factor was rather small ($p\text{-value} > 0.01$). Figure 7a displays the in-line SFV data of batches 6 (50°C drying temperature) and 14 (70°C drying temperature) to highlight the effect of the drying temperature on the granulation process. The other settings are the same for both batches. The plot shows that both batches had approximately the same particle size (same start process conditions) at the start of the drying period, but that batch 6, which was dried at a lower temperature for a longer period, resulted in crumbled granules having a smaller end granule particle size.

Figure 7b also displays 2 batches with different drying conditions (batch 1 was dried at 50°C and batch 9 at 70°C). Although both batches had initially the same process conditions, after the spraying period they did not have the same particle size which was possibly due to inappropriate fluidization influencing the agglomeration process. Furthermore, there was a clear difference in particle size evolution during drying between batch 1 and 9 (the longer drying period at the lower temperature level of batch 1 caused more attrition of the granules and thus a larger decrease in particle size during the drying period), nevertheless they resulted in similar end granule sizes, used to calculate DOE models. Hence, for both batches the similar response variables were used in the DOE, despite the fact that both batches had a very different process progress. The different applied inlet air temperature during drying clearly affects the drying process of batch 1 and 9. However, this is not transposed in the end product particle size (response variable used for the DOE analysis) as the batches did not have the same particle size at the start of the drying period. This might explain why the drying temperature was of limited significance according to the DOE. Only the continuous in-line obtained information from the SFV probe was able to give this in-depth understanding.

The data in figures 7a and 7b also displays another process phenomenon: shaking of the filter bags. At the beginning of all processes, powders had a small particle size as almost no binder liquid was added yet. As result, the powder particles got trapped into the filter bags. These bags were shaken every 45 s, releasing the small particles which were hence passing the probe, causing a drop in measured particle size after each shaking period. As the granulation process progressed, more binder liquid was sprayed and these small particles were agglomerated into larger granules. Hence, less particles were trapped into the bags

resulting in less fluctuations in the particle size versus process time plots. During the drying phase of each granulation process, granules could be attrited depending on the process conditions and the smaller particles could get entrapped again into the filter bags, causing a drop in particle size (see drying period of batch 1 in figure 7b) after shaking of the bags each time. This proves that the in-line SFV probe was sensitive to all sudden changes in particle size during granulation processes.

Influence of inlet air temperature during spraying

The results of the performed DOE showed that the inlet air temperature during spraying has no significant effect upon the end granule size.

Figure 8 gives an example of the in-line SFV data during the spraying phase of 2 batches where a different spraying temperature was used. During the agglomeration period of batch 5 (with a spraying temperature of 50°C), there was a higher variability of the particle size compared to batch 1 (with a spraying temperature of 40°C), due to the continuous entrapment of small particles in and subsequent discharge from the filter bags. Small particles were longer present in batch 5 than in batch 1 as the agglomeration occurred slower in batch 5 due to the faster evaporation of binder liquid at the upper temperature level. However, at the end of the spraying period, a similar particle size was observed at both levels, indicating that the influence of the inlet air temperature during spraying was not pronounced enough to create a difference in particle size at the end of the spraying period.

Influence of Tween on granule size

According to the performed DOE, the amount of Tween 20 has no significant effect upon particle size. The in-line SFV data profiles of the batches having different Tween 20 settings but having identical settings for the other examined variables were always similar.

3.2.3 Influence of DOE factors upon density and powder flow

Particle size distribution is one of the most important characteristics of granules, but other properties, such as density and flowability are also of importance for further processing. These latter properties were determined as described in section 2.5, and it was examined which of the examined DOE variables had a significant effect upon these properties (see table 5). Based on the MODDE software models and the calculated half-normal plots (with algorithm of Dong), similar conclusions were made.

Tapped density DOE model

HPMC concentration and *inlet air temperature during drying* have the largest significant negative effect upon tapped density, indicating that by increasing these factors the density of the granules decreases. These effects can be explained by the results in section 3.2.1. The SFV DOE model shows that increasing the amount of HPMC and increasing the drying temperature creates larger granules. These larger granules are less cohesive and occupy more volume, thus decreasing the density of the granules.

According to table 5, the *inlet air temperature during spraying* has also a significant negative effect upon tapped density, although with a smaller significance compared to the HPMC concentration and the inlet air temperature during drying. The SFV DOE model showed that the spraying temperature does not significantly influence the particle size of granules. Hence, the negative effect on density is not caused by a larger volume (larger particle size).

Hausner ratio DOE model

The granules had passable, fair or good flow characteristics according to the scale of flowability, based on the calculated Hausner ratio. The DOE model (table 5) shows that only the HPMC concentration significantly negatively affects Hausner ratios, indicating that increasing the amount of HPMC, reduces the values of this index, thus increasing the flowability of the granules. The explanation was found in the results of the SFV (or LD) model: more HPMC in the binder liquid creates larger granules which reduces the cohesiveness of the granules, thus increasing flow properties.

3.2.4 Assessment of granule density and flowability from in-line SFV measurements

In the final part of this study, it was examined whether the density and flowability of the 19 DOE experiments could be related to the in-line SFV determined particle size distributions as these granule properties are closely related to the particle size distribution (see 3.2.3). Univariate, multivariate and multiway approaches were considered (with the tapped density and the Hausner ratio values of the 19 DOE batches as dependent variables: 19 x 1 Y-vector). Independent models were built for tapped density and Hausner ratio.

- **Univariate:** A *linear* model was built using the *D50* SFV values of the end granules of the 19 DOE experiments as independent variables (19 x 1 X-vector).
- **Multivariate:** A *partial least squares (PLS)* model was built using the *D01, D10, D25, D50, D63, D75, D90 and D99* SFV values of the end granules of the 19 DOE experiments as independent variables (19 x 8 X-matrix).
- **Multiway:** A *N-way partial least squares (N-PLS)* model was built using the *D01, D10, D25, D50, D63, D75, D90 and D99* SFV values of the 19 DOE experiments *in function of complete batch time* as independent variables (3-way X-matrix).

The quality of the models was compared by evaluation of R^2 (explained variance) and RMSEE (root mean square error of estimation, Eq. (1)) values. R^2 reflects the goodness of fit and the RMSEE specifies the root mean square error of the fit for observations in the work set, hence giving a direct indication of the error in the model (adjusted to the scale of the model):

$$RMSEE = \sqrt{\frac{\sum_{i=1}^N (y_{iobs} - y_{ipred})^2}{N-A-1}} \quad \text{Eq. (1)}$$

N = number of experiments, y_{iobs} = observed Y-value, y_{ipred} = predicted Y-value according to the model, A = number of PLS components in the model

According to table 6, the multivariate PLS tapped density model and the multiway N-PLS Hausner ratio model have the highest R^2 values in combination with the lowest RMSEE values. For tapped density, the use of a multivariate approach seemed justified as the correlation improved by more than 10%. In case of the Hausner ratio models, the benefits of a more complicated multivariate or multiway approach was not as pronounced, as the amount of variance explained by the model did not increase largely. This might be explained by the fact that when going from a univariate (only based on *D50* values) to a multivariate model (use of 8 different *D*-values), all *D*-values express similar granule size distributions as the granules had similar deviations around their average particle size for all batches (i.e., all *D*-values carry similar information). Furthermore, the determined granule properties mainly

depend on the end granule particle size distribution and not on the particle size distribution of the start materials, which is used in the multiway model, and early process materials.

As the errors of the models were rather small, the results suggest that the models had a good prediction ability and the in-line SFV data can give an indication towards the magnitude of the off-line measured end granule properties. Nevertheless, the model performance should be tested on an independent test set as the RMSEE values relate to the errors within the calibration set and may overestimate the actual model performance.

4. Conclusions

In this study, the use of in-line SFV as PAT monitoring tool for particle growth during fluid bed granulation was evaluated. Comparison between in-line SFV and off-line LD data demonstrated that an identical trend in D50 values among all different monitored batches was obtained by both methods, although in-line obtained granule sizes were always larger than the corresponding off-line LD results, due to the measurement method of LD. The in-line SFV data did not underestimate the actual granule size due to size segregation and no probe fouling occurred during any of the granulations. These results suggest that SFV data were reliable and representative to the actual particle size.

Analysis of the SFV and LD DOE models showed that the HPMC concentration had the most significant (positive) effect upon the particle size of the granules. The influence of the inlet air temperature during drying was smaller in comparison. The in-line SFV probe provided every 10 s information about the granulation process, which allowed to explain and better understand the (in)significance of the studied variables upon granulation, which was not possible using the off-line LD data.

The influence of the DOE variables on density and flow properties of the granules could be explained by the results of the in-line SFV DOE model. The multivariate PLS tapped density model and the multiway N-PLS Hausner ratio model, built to assess these properties during processing, had the highest R^2 values in combination with the lowest RMSEE values.

The results suggest that in-line SFV technology is a good PAT monitoring tool which is sensitive to any particle size changes during granulation and which helps to increase granulation process understanding. This indicates the potential use of the SFV technique during different stages in the development process of new drug molecules. Moreover, the continuous and rapid measurement of particle size distribution during the granulation process, enables the possibility to improve process quality and increase the efficiency and control of the production process.

The results also indicate the ability to predict end granule properties based on SFV data which can be beneficial in both development and routine production. Nevertheless, the full use of such an approach requires further testing of model performance on an independent test set as the RMSEE values may overestimate the actual model performance.

Acknowledgement

This work was financially supported by the Institute for the Promotion of Innovation through Science and Technology in Flanders (IWT-Vlaanderen).

References

- [1] S.M. Iveson, J.D. Litster, K. Hapgood, B.J. Ennis, Nucleation, growth and breakage phenomena in agitated wet granulation processes: a review, *Powder Technol.* 117 (2001) 3-39.
- [2] Food and Drug Administration, Process Analytical Technology Initiative, Guidance for Industry PAT - A Framework for Innovative Pharmaceutical development, Manufacturing and Quality Assurance (2004).
- [3] International Conference on Harmonisation, Guidance for Industry, Q8(R1) Pharmaceutical Development (2009).
- [4] S. Watano, K. Miyanami, Image-processing for online monitoring of granule size distribution and shape in fluidized-bed granulation, *Powder Technol.* 83 (1995) 55-60.
- [5] S. Watano, Y. Sato, K. Miyanami, Control of granule growth in fluidized bed granulation by an image processing system, *Chem. Pharm. Bull.* 44 (1996) 1556-1560.
- [6] S. Watano, Y. Sato, K. Miyanami, Optimization and validation of an image processing system in fluidized bed granulation, *Adv. Powder Technol.* 8 (1997) 269-277.
- [7] S. Watano, T. Numa, K. Miyanami, Y. Osako, On-line monitoring of granule growth in high shear granulation by an image processing system, *Chem. Pharm. Bull.* 48 (2000) 1154-1159.
- [8] S. Watano, Direct control of wet granulation processes by image processing system, *Powder Technol.* 117 (2001) 163-172.
- [9] S. Watano, T. Numa, K. Miyanami, Y. Osako, A fuzzy control system of high shear granulation using image processing, *Powder Technol.* 115 (2001) 124-130.
- [10] T. Naervanen, K. Seppaelae, O. Antikainen, J. Yliruusi, A new rapid on-line imaging method to determine particle size distribution of granules, *AAPS PharmSciTech* 9 (2008) 282-287.
- [11] P. Frake, D. Greenhalgh, S.M. Grierson, J.M. Hempenstall, D.R. Rudd, Process control and end-point determination of a fluid bed granulation by application of near infra-red spectroscopy, *Int. J. Pharm.* 151 (1997) 75-80.
- [12] S.G. Goebel, K.J. Steffens, Online-measurement of moisture and particle size in the fluidized-bed processing with the near-infrared spectroscopy, *Pharm. Ind.* 60 (1998) 889-895.
- [13] W.P. Findlay, G.R. Peck, K.R. Morris, Determination of fluidized bed granulation end point using near-infrared spectroscopy and phenomenological analysis, *J. Pharm. Sci.* 94 (2005) 604-612.
- [14] P. Luukkonen, M. Fransson, I.N. Bjorn, J. Hautala, B. Lagerholm, S. Folestad, Real-time assessment of granule and tablet properties using in-line data from a high-shear granulation process, *J. Pharm. Sci.* 97 (2008) 950-959.
- [15] A. Tok, X.P. Goh, W. Ng, R. Tan, Monitoring Granulation Rate Processes Using Three PAT Tools in a Pilot-Scale Fluidized Bed, *AAPS PharmSciTech* 9 (2008) 1083-1091.
- [16] A.A. Kaddour, B. Cuq, In-line monitoring of wet agglomeration of wheat flour using near infrared spectroscopy, *Powder Technol.* 190 (2009) 10-18.
- [17] X.H. Hu, J.C. Cunningham, D. Winstead, Study growth kinetics in fluidized bed granulation with at-line FBRM, *Int. J. Pharm.* 347 (2008) 54-61.
- [18] M. Whitaker, G.R. Baker, J. Westrup, P.A. Goulding, D.R. Rudd, R.M. Belchamber, M.P. Collins, Application of acoustic emission to the monitoring and end point determination of a high shear granulation process, *Int. J. Pharm.* 205 (2000) 79-91.
- [19] M. Halstensen, P. de Bakker, K.H. Esbensen, Acoustic chemometric monitoring of an industrial granulation production process - a PAT feasibility study, *Chemometrics Intell. Lab. Syst.* 84 (2006) 88-97.
- [20] J.F. Gamble, A.B. Dennis, M. Tobyn, Monitoring and end-point prediction of a small scale wet granulation process using acoustic emission, *Pharm. Dev. Technol.* 14 (2009) 299-304.
- [21] S. Matero, S. Poutiainen, J. Leskinen, K. Jarvinen, J. Ketolainen, S.P. Reinikainen, M. Hakulinen, R. Lappalainen, A. Poso, The feasibility of using acoustic emissions for monitoring of fluidized bed granulation, *Chemometrics Intell. Lab. Syst.* 97 (2009) 75-81.

- [22] D. Petrak, Simultaneous measurement of particle size and particle velocity by the spatial filtering technique, *Part. Part. Syst. Charact.* 19 (2002) 391-400.
- [23] D. Petrak, H. Rauh, Optical probe for the in-line determination of particle shape, size, and velocity, *Part. Sci. Technol.* 24 (2006) 381-394.
- [24] S. Schmidt-Lehr, H.U. Moritz, K.C. Jurgens, Online-control of the particle size during fluid-bed granulation/evaluation of a novel laser probe for a better control of particle size in fluid-bed granulation, *Pharm. Ind.* 69 (2007) 478-484.
- [25] T. Narvanen, T. Lipsanen, O. Antikainen, H. Raikkonen, J. Yliruusi, Controlling granule size by granulation liquid feed pulsing, *Int. J. Pharm.* 357 (2008) 132-138.
- [26] T. Narvanen, T. Lipsanen, O. Antikainen, H. Raikkonen, J. Heinamaki, J. Yliruusi, Gaining Fluid Bed Process Understanding by In-Line Particle Size Analysis, *J. Pharm. Sci.* 98 (2009) 1110-1117.
- [27] T. Lipsanen, T. Narvanen, H. Raikkonen, O. Antikainen, and J. Yliruusi, Particle Size, Moisture, and Fluidization Variations Described by Indirect In-line Physical Measurements of Fluid Bed Granulation, *AAPS PharmSciTech* 9 (2008) 1070-1077.
- [28] Y. Vander Heyden, A. Nijhuis, J. Smeyers-Verbeke, B.G.M. Vandeginste, D.L. Massart, Guidance for robustness/ruggedness tests in method validation, *J. Pharm. Biomed. Anal.* 24 (2001) 723-753.

- Figure 1. Fluid bed granulator with in-line SFV probe (probe at a height of 20 cm and depth of 5 cm)
- Figure 2. Comparison between the D50 results obtained with in-line SFV and off-line LD for all DOE batches
- Figure 3. Differences between the D10 (red circles), the D50 (blue squares) and the D90 results (green triangles) of the SFV and LD measurements for the 19 DOE batches
- Figure 4. Differences between D50 values of SFV and LD
Figure 4a. Differences between D50 values of SFV and LD arranged (x-axis) according to increasing SFV particle size
Figure 4b. Differences between D50 values of SFV and LD arranged (x-axis) according to increasing LD particle size
- Figure 5. Half-normal plots
Figure 5a. Half-normal plot of SFV results with critical margin of error (A = HPMC concentration, B = Tween 20 concentration, C = inlet air T during spraying, D = inlet air T during drying)
Figure 5b. Half-normal plot of LD results with critical margin of error (A = HPMC concentration, B = Tween 20 concentration, C = inlet air T during spraying, D = inlet air T during drying)
- Figure 6. In-line SFV data of batches 13/14 (1%/3% HPMC, 0.2% Tween 20, 50°C spraying T, 70°C drying T) with 1: end of spraying phase and 2: end of drying phase
- Figure 7. In-line SFV data of batches with a different drying T
Figure 7a. In-line SFV data of batches 6/14 (3% HPMC, 0.2% Tween 20, 50°C spraying T, 50°C/70°C drying T)
Figure 7b. In-line SFV data of batches 1/9 (1% HPMC, 0.2% Tween 20, 40°C spraying T, 50°C/70°C drying T)
- Figure 8. In-line SFV data during spraying phase of batches 1/5 (1% HPMC, 0.2% Tween 20, 40°C/50°C spraying T, 50°C drying T)

Figure 1.

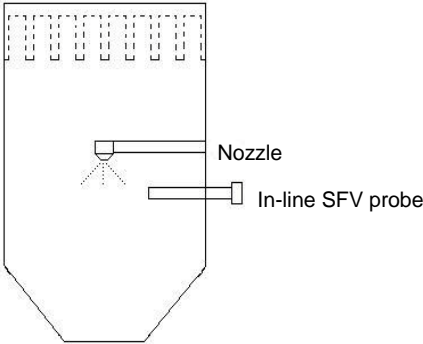


Figure 2

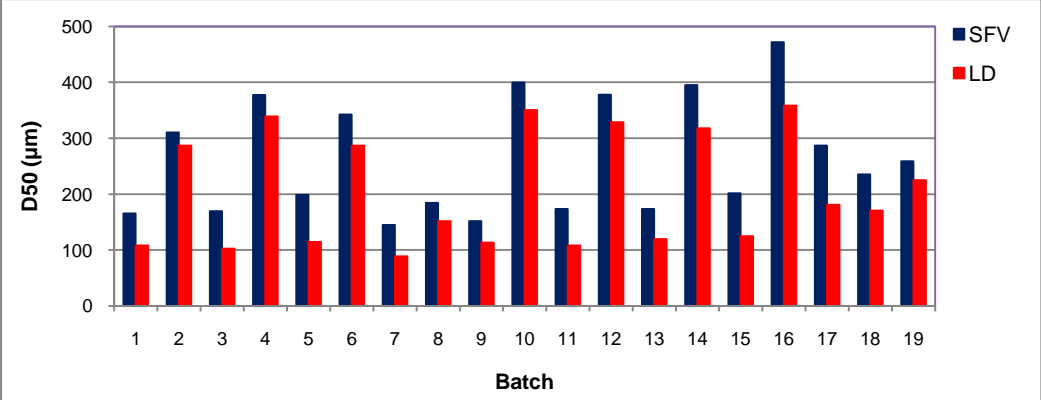


Figure 3.

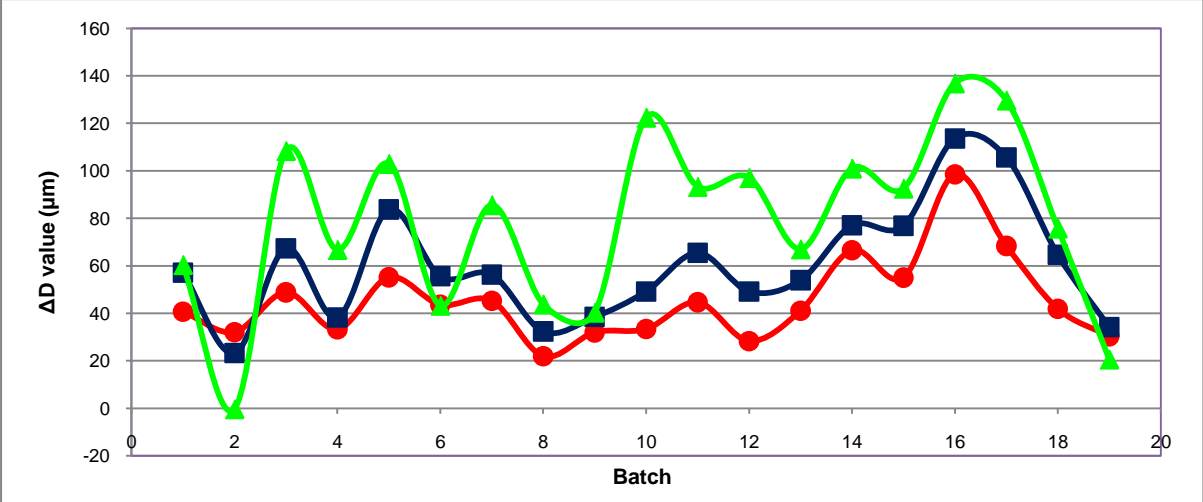


Figure 4a.

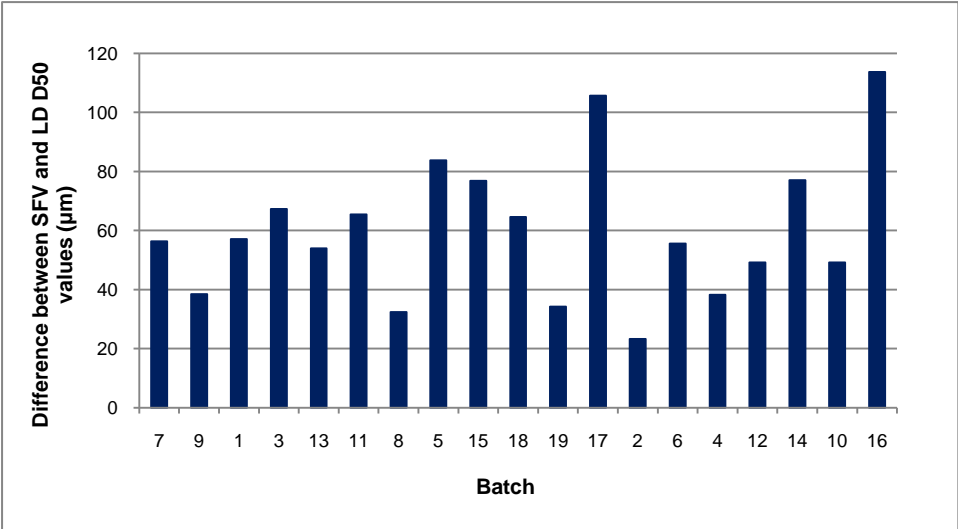


Figure 4b.

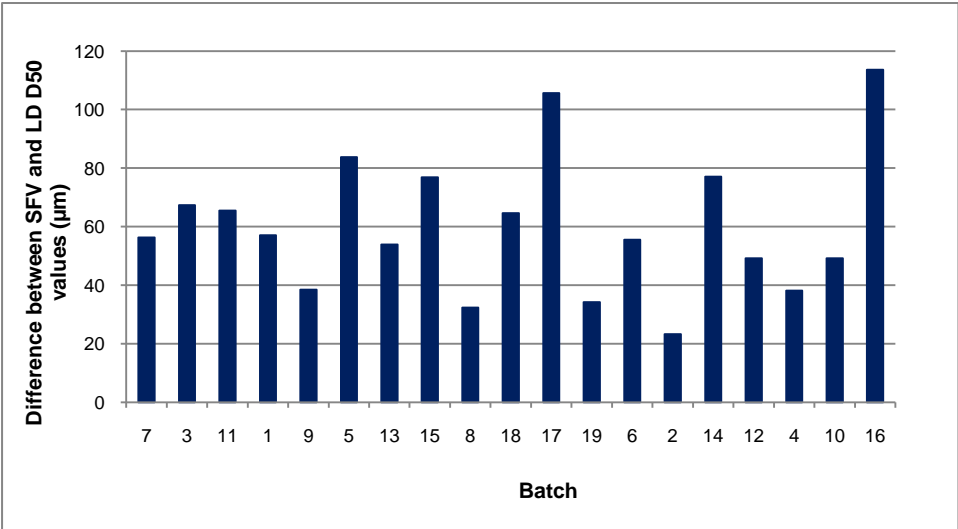


Figure 5a.

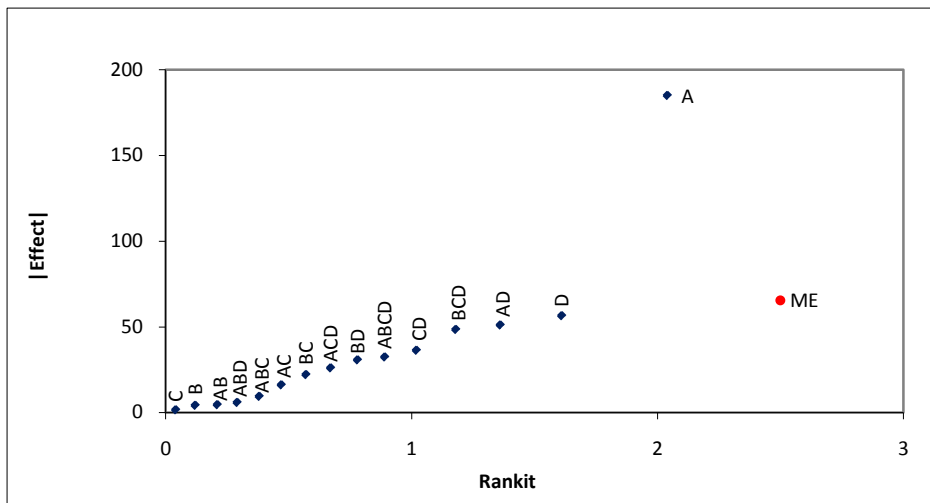


Figure 5b.

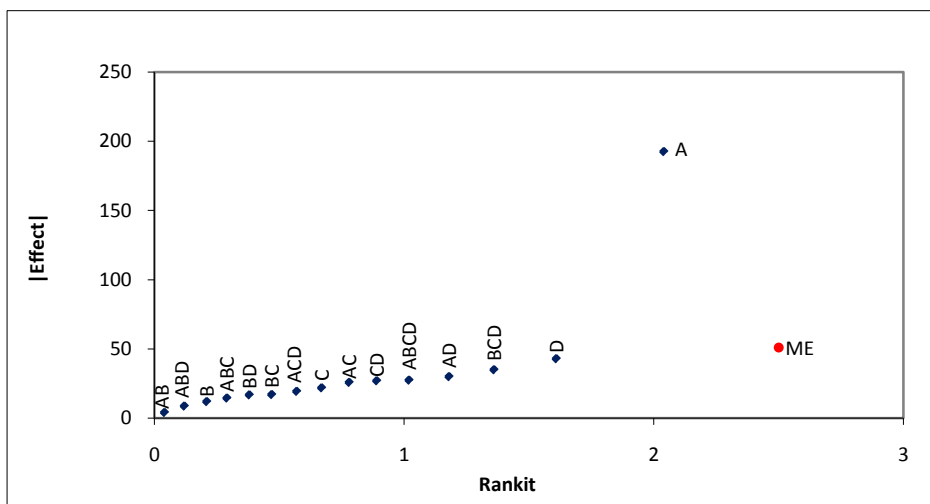


Figure 6.

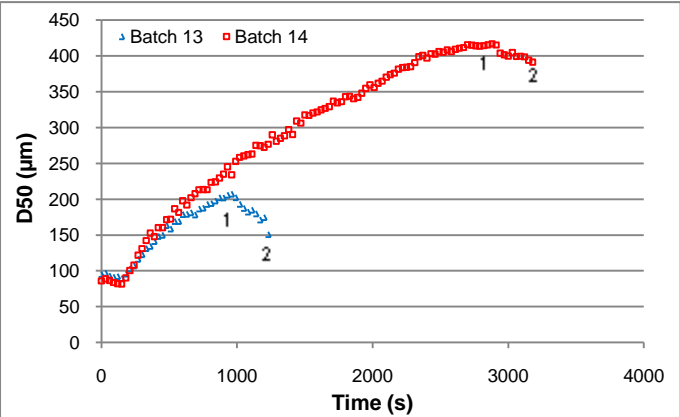


Figure 7a.

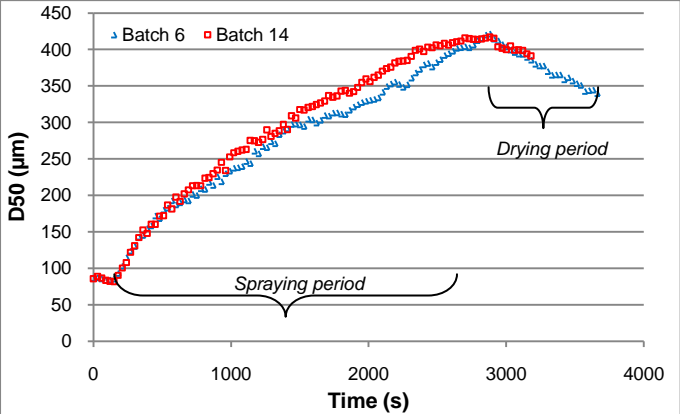


Figure 7b.

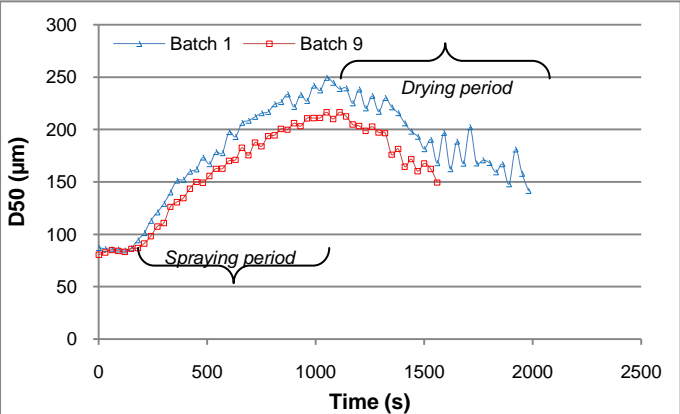


Figure 8.

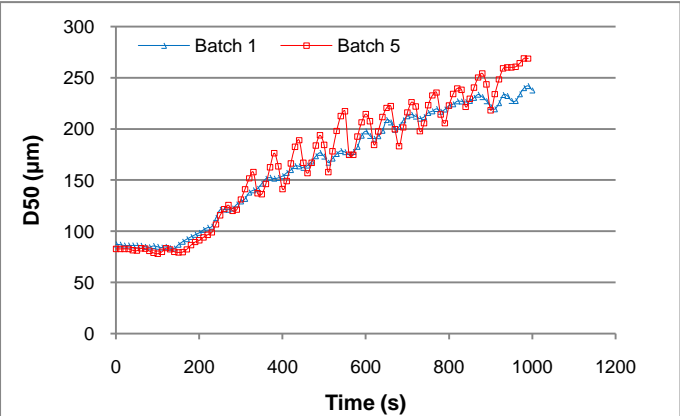


Table 1. Design matrix 2-level full factorial design

<i>Batch</i>	<i>HPMC</i>	<i>Tween 20</i>	<i>Inlet air T during spraying</i>	<i>Inlet air T during drying</i>
1	-1	-1	-1	-1
2	1	-1	-1	-1
3	-1	1	-1	-1
4	1	1	-1	-1
5	-1	-1	1	-1
6	1	-1	1	-1
7	-1	1	1	-1
8	1	1	1	-1
9	-1	-1	-1	1
10	1	-1	-1	1
11	-1	1	-1	1
12	1	1	-1	1
13	-1	-1	1	1
14	1	-1	1	1
15	-1	1	1	1
16	1	1	1	1
17	0	0	0	0
18	0	0	0	0
19	0	0	0	0

Table 2. Levels of examined variables

<i>Variable</i>	<i>Unit</i>	<i>Lower level</i>	<i>Upper level</i>
<i>HPMC</i>	%w/w	1	3
<i>Tween 20</i>	%w/w	0.2	0.3
<i>Inlet air T during spraying</i>	°C	40	50
<i>Inlet air T during drying</i>	°C	50	70

Table 3. R^2 and Q^2 values of SFV and LD based models

	<i>SFV</i>	<i>LD</i>
R^2	0.84	0.87
Q^2	0.73	0.79

Table 4. Statistical significance (p) of coefficients in SFV and LD based models

	<i>SFV</i>		<i>LD</i>	
	<i>Coefficient</i>	<i>p</i>	<i>Coefficient</i>	<i>p</i>
<i>HPMC</i>	92.5	***	96.3	***
<i>T_{drying}</i>	28.3	*	21.4	*
<i>HPMC*T_{drying}</i>	25.6	*	15.0	NS

*p<0.05, **p<0.01, ***p<0.001, NS = not statistically significant

Table 5. Statistical significance (p) of coefficients in tapped density and Hausner ratio DOE models

	<i>Tapped Density</i>		<i>Hausner Ratio</i>	
	<i>Coefficient</i>	<i>p</i>	<i>Coefficient</i>	<i>p</i>
<i>HPMC</i>	-0.0522	***	-0.0238	**
<i>Tween</i>	0.0040	NS	0.0113	NS
<i>T_{spraying}</i>	-0.0156	**	0.0113	NS
<i>T_{drying}</i>	-0.0270	***	-0.0025	NS
<i>HPMC*Tween</i>	-0.0016	NS	0.0025	NS
<i>HPMC*T_{spraying}</i>	-0.0043	NS	0.0175	*
<i>HPMC*T_{drying}</i>	0.0044	NS	0.0012	NS
<i>Tween*T_{spraying}</i>	0.0116	*	0.0125	NS
<i>Tween*T_{drying}</i>	-0.0013	NS	-0.0037	NS
<i>T_{spraying}*T_{drying}</i>	0.0008	NS	-0.0062	NS

*p<0.05, **p<0.01, ***p<0.001, NS = not statistically significant

Table 6. RMSEE and R^2 values of univariate, multivariate and multiway tapped density and Hausner ratio models with the mean and standard deviation of actually measured properties

	<i>Univariate</i>		<i>Multivariate (PLS)</i>		<i>Multiway (N-PLS)</i>		<i>Mean</i>	<i>St.Dev.</i>
	<i>RMSEE</i>	<i>R² (%)</i>	<i>RMSEE</i>	<i>R² (%)</i>	<i>RMSEE</i>	<i>R² (%)</i>		
<i>Tapped density</i>	0.0339	69	<u>0.0279</u>	<u>82</u>	0.0360	70	0.53	0.059
<i>Hausner ratio</i>	0.0307	46	0.0281	47	<u>0.0268</u>	<u>52</u>	1.21	0.037